1

Dependence of precipitation on precipitable water vapor over the Maritime Continent and implications to the Madden-Julian Oscillation

4

Siyue Chen[1,2], Nathanael Z. Wong[2], Ding Ma[2], Pak Wah Chan[2]†, Zhiming Kuang[2,3]

[1]Department of Atmospheric and Oceanic Sciences, School of Physics, Peking University, Beijing, China.

[2]Department of Earth and Planetary Sciences, Harvard University, Cambridge, MA, USA.

[3]John A. Paulson School of Engineering and Applied Sciences, Harvard University, Cambridge, MA, USA.

†Now at College of Engineering, Mathematics and Physical Sciences, University of Exeter, Exeter, UK.

13

Corresponding author: Siyue Chen (siyue_chen@fas.harvard.edu)

15

16

Key Points:

- The dependence of precipitation on precipitable water vapor is stronger over ocean than over the Maritime Continent.
- The MJO modulates the precipitable water vapor over the ocean and over the Maritime Continent by roughly the same amount.
- Weaker precipitation variations over the Maritime Continent between the MJO phases may be explained by the weaker water vapor dependence.

24

Abstract

The weakening of the Madden-Julian Oscillation (MJO) as it propagates over the Maritime Continent (MC) is often referred to as the MC barrier. Here, we use 3-hourly precipitable water vapor (PWV) data obtained from the Sumatran GPS Array and the ERA5 reanalysis to investigate the role played by the column moisture over the MC. Over Sumatra and the whole MC, we find a stronger dependence of precipitation on PWV over the ocean as compared to both inland and coastal regions. The MJO modulates the PWV over the ocean and over the MC by roughly the same amount, and the weaker precipitation variations over the MC between the MJO phases may be interpreted in terms of its weaker dependence on PWV over the MC. This different precipitation dependence on column moisture between the MC and the ocean may contribute to the MC barrier effect.

Plain Language Summary

The Madden-Julian Oscillation (MJO) is the dominant intraseasonal variability in the tropical atmosphere, and also influences the global climate and weather, including the El Nino-Southern Oscillation and the North Atlantic Oscillation. However, the reason behind why the MJO weakens or terminates as it propagates over the Maritime Continent remains unclear. Based on the idea that the rainfall is highly sensitive to the water vapor in the troposphere, we examine observations and reanalysis data. We find a weaker dependence of rainfall on column water vapor over the Maritime Continent than over the oceans, which may provide a simple interpretation of the smaller changes of rainfall over land associated with the MJO.

1 Introduction

The Madden-Julian Oscillation (MJO) is the dominant component of the intraseasonal (30-90 days) variability in the tropical atmosphere (Madden & Julian, 1971, 1972). In a typical MJO event, a convectively active envelope of precipitation develops over the western Indian Ocean and slowly propagates eastward along equator to the Pacific Ocean. Over the past decades, there have been extensive studies into both the mechanisms of the MJO and its interaction with the extratropical weather, and other large-scale modes of variability [e.g. the Asian monsoon, the El Nino-Southern Oscillation (ENSO), the North Atlantic Oscillation (NAO), etc.] (Kiladis & Weickmann, 1992; Mo, 2000; Zhang, 2005; Schreck et al., 2013; Zhou et al., 2016; Tippett, 2018; Barrett, 2019; Arcodia et al., 2020).

The Maritime Continent (MC) is a region in the tropics dominated by islands, many of which fall along the path of the MJO (Yamanaka, 2016). The MJO acts to modulate the rainfall and local land-sea circulation over the MC (Tian et al., 2006; Fujita et al., 2011). Recent observational analysis shows that the MC appears to be a barrier to the MJO propagation – some MJO events become weaker over the MC as they propagate into Pacific Ocean, while some terminate over the MC (Rui & Wang, 1990; Zhang & Ling, 2017). Model simulations show relatively low skills in representing this barrier effect (Inness et al., 2003; Seo et al., 2009; Vitart & Molteni, 2010; Weaver et al., 2011;Wang et al., 2019). Rainfall variance associated with the MJO is also markedly lower over the islands compared to their surrounding oceans (Maloney & Sobel, 2004).

Previously proposed mechanisms for this barrier effect involve, for example, local orography and the strong diurnal cycle over land. Maloney & Sobel (2004) attributed the smaller MJO modulation of the rainfall over the islands to the fact that land surfaces have lower sensible

68 and latent heat capacity compared to the open ocean. Inness & Slingo (2006) and Wu & Hsu
69 (2009) suggested that the elevated orography over the islands could act to block the propagation
70 of low-level pressure and wind signal, which may disrupt the MJO propagation. Previous studies
71 have also attributed the weakening of the MJO over the MC to the strong diurnal cycle over land
72 and related phenomena (Neale & Slingo, 2003; Rauniyar & Walsh, 2011; Hagos et al., 2016;
73 Majda & Yang, 2016). For example, the strong diurnal cycle of convection over islands increases
74 the cloud cover and decreases surface insolation, which results in the lower precipitation rate
75 over land in the MC (Rauniyar & Walsh, 2011). After removing the diurnal cycle of the
76 incoming shortwave radiation at the top of the atmosphere, it was found through numerical
77 simulations of a MJO event that the MJO could propagate more smoothly through the MC
78 (Hagos et al., 2016).

79 Our work is motivated by the possibility of interpreting this barrier effect of the MC in
80 the "moisture mode" framework for the MJO (e.g. Raymond, 2001; Andersen & Kuang, 2012;
81 Sobel & Maloney, 2012, 2013; Adames & Kim, 2016). The "moisture mode" framework
82 postulates that the MJO arises from a positive feedback in which an anomalously moist
83 atmospheric column precipitates more, and the combined effect of anomalous radiative and
84 surface fluxes and anomalous advection due to the resulting circulation further leads to an even
85 moister column, resulting in a positive feedback loop.

86 Based on the daily rainfall and PWV derived from microwave measurements, Bretherton
87 et al. (2004) showed an exponential relationship between rainfall and PWV over different
88 tropical ocean areas, which may be interpreted as an empirical (and partial) support for the
89 "moisture mode" framework. Within this framework, if the dependence of precipitation on PWV
90 is weaker over the MC, e.g., due to a strong diurnal cycle, this weaker dependence may lead to a
91 weaker "moisture mode" and contribute to the barrier effect.

92 It has been previously established with Tropical Rainfall Measuring Mission (TRMM)
93 rainfall measurements that modulation of rainfall by the MJO is weaker over the MC compared
94 to that over the surrounding oceans (Maloney & Sobel, 2004; Sakaeda et al., 2017). PWV over
95 the MC is not available from the microwave measurements used in Bretherton et al. (2004)
96 owing to the complications associated with land-surface emissivity. Roundy & Frank (2004)
97 used data from the NASA Water Vapor Project (NVAP), but the data may be problematic over
98 the MC (Torri et al., 2019). Bergemann & Jakob (2016) used the ERA-Interim data from 1998 to
99 2015 to study the rainfall-PWV relationship and found that coastally influence rainfall has a
100 weaker dependence on mid-troposphere humidity than that over the open ocean. However, the
101 accuracy of the ERA-Interim water vapor data over the Maritime Continent has not been well
102 established, and over a substantial portion of the dataset time period, all-weather data such as
103 that from GPS Radio Occultation was not available for assimilation. Torri et al. (2019) used data
104 from the Sumatran GPS Array (SuGAr), a network of ground GPS stations in Sumatra
105 established for geodesic studies (Feng et al., 2015), and found that the MJO modulates the
106 diurnally averaged PWV over the archipelago and coastal stations by similar amounts (Fig. 12 in
107 Torri et al. (2019)). If we take the coastal stations to be more land-like than the archipelago
108 stations, these results imply a weaker dependence of rainfall on PWV over the different MJO
109 phases over Sumatra.

110 In our work, we extend the work by Torri et al. (2019) in two ways. We first examine the
111 dependence of rainfall on PWV more generally in a manner following the approach of
112 Bretherton et al. (2004). Second, in addition to Sumatra, we extend the analysis to the entire MC

113 region using ERA5 reanalysis data (Hersbach et al., 2020), which assimilates GPS radio
114 occultation (RO) data. The GPS RO data show a good agreement with collocated ground-based
115 GPS measurements in Torri et al. (2019)'s Fig.5. This work also revisits Bergemann & Jakob
116 (2016) and Ahmed & Schumacher (2017) using the SuGAr dataset and the new ERA5 data. The
117 comparison between reanalysis PWV and co-located SuGAr data (Figure 1bc) shows that ERA5
118 has improved quality compared to ERA-Interim used in the previous work. Also, we divided the
119 Maritime Continent into 4 geographic categories in order to investigate the change in rain-PWV
120 relationship over different regions in more detail, while the MC is regarded as a whole in Ahmed
121 & Schumacher (2017).

122   In section 2, we will introduce the datasets and methods. In subsections 3.1 and 3.2, we
123 will present the results of the diurnal cycle of rainfall and PWV and relationship between rainfall
124 and PWV. In subsection 3.3, we will investigate how the MJO modulates the PWV and rainfall
125 over MC, and their linkage. In section 4, we will summarize the results and interpret the MC
126 barrier effect using our findings.

127 **2 Data and Methods**

128   In this work, PWV is estimated using ground-based GPS-derived network data over
129 Sumatra and ERA5 reanalysis over the Maritime Continent. We also use the Global precipitation
130 measurement (GPM) rainfall data.

131   2.1 PWV data from Sumatra GPS Array station (SuGAr)

132   GPS relies on the transmission of radio wave signals from satellite to receiver in order to
133 obtain precise positions. When these signals travel through the atmosphere, two potential sources
134 of error arise due to refraction of the radio waves – the ionospheric delay, and the tropospheric
135 delay. The delay due to the tropospheric component (tropospheric path delay) in the neutral
136 atmosphere (troposphere and stratosphere) can be further divided into the hydrostatic delay and
137 the wet delay, the latter of which, when mapped to the zenith angle, can be used to obtain
138 precipitable water data (Askne & Nordius, 1987). The relative insensitivity of L-band radio
139 signals to cloud and droplet makes the GPS-PWV product available in all weather conditions. In
140 our study, as in Torri et al. (2019)**,** we use data from 45 GPS stations over Sumatra during the
141 period of 2008-2013 (Feng et al., 2015). We divide the stations into three categories: the small
142 islands west of Sumatra (ocean), the coast along Sumatra (coast), and inland (land) as shown in
143 Fig. 1a.

144   2.2 PWV data over the MC from ERA5 reanalysis

145   As for the PWV data over the broader Maritime Continent (10°S-10°N, 90°E-150°E), we
146 utilize ERA5, the latest global atmospheric reanalysis dataset released by the European Centre
147 for Medium-range Weather Forecasts. The Constellation Observing System for Meteorology,
148 Ionosphere, and Climate Version 1&2 (COSMIC1&2) radio occultation measurements, which
149 can provide information on temperature and humidity based on the signal refraction, were
150 assimilated into ERA5 since 2006 and 2020, respectively. The ERA5 reanalysis PWV data
151 compare well with COSMIC1&2 over the Maritime Continent (Fig. S1) and provide a better
152 temporal and spatial coverage. Therefore, we use ERA5 PWV data whose time resolution is 1
153 hour, and spatial resolution is 0.25°, over the Maritime Continent during 2005-2016. Based on
154 ERA5 land fraction data, we divide the Maritime Continent area into ocean (land fraction<0.1),

155 coast (0.1<land fraction<0.8) and land (land fraction>0.8) grids, which is similar to the three
156 categories of SuGAr stations. As PWV is the integral of column of water vapor above the
157 ground, a higher elevation means a shorter integration path and a naturally lower PWV value.
158 Therefore, we exclude grids where the elevation is higher than 150 meters from the three
159 categories above and reclassify them as mountainous regions, so that regions remain classified as
160 "land" and "coast" can better compare with the "ocean".

161   2.3 Rainfall data from Global Precipitation Measurement

162   The Global Precipitation Measurement (GPM) is the successor to TRMM. It has two
163 advanced instruments, Dual-frequency Precipitation Radar and a radiometer called GPM
164 Microwave Imager, which allows GPM to measure precipitation intensity and type through all
165 cloud layers using a wider data swath (Oda et al., 2019). The Integrated Multi-Satellite
166 Retrievals for GPM (IMERGv6) we use here, is the Level 3 precipitation estimation product of
167 GPM, which intercalibrate, merge, and interpolate satellite microwave precipitation estimates
168 with microwave calibrated infrared (IR) satellite estimates, precipitation gauge analyses at
169 high spatio-temporal resolution of 30 minutes and 0.1°. In order to do a comparison with the
170 PWV data, we average the higher-resolution GPM 0.1° by 0.1º data to a coarser 0.25º by 0.25°
171 grid exported by the ERA5 reanalysis.

172   2.4 RMM MJO index

173   Wheeler and Hendon (2004) developed the Real-time Multivariate MJO (RMM) index to
174 compute the state of the MJO using latitudinal averages of outgoing longwave radiation and
175 zonal wind at 200 and 850 hPa in the tropics. This index has become the standard method used to
176 describe the approximate center and phase of the MJO as it propagates along the equator. Based
177 on the rainfall (Fig. S4), we assign RMM MJO phases 2, 3, 4, 5 as active MJO phases and phases
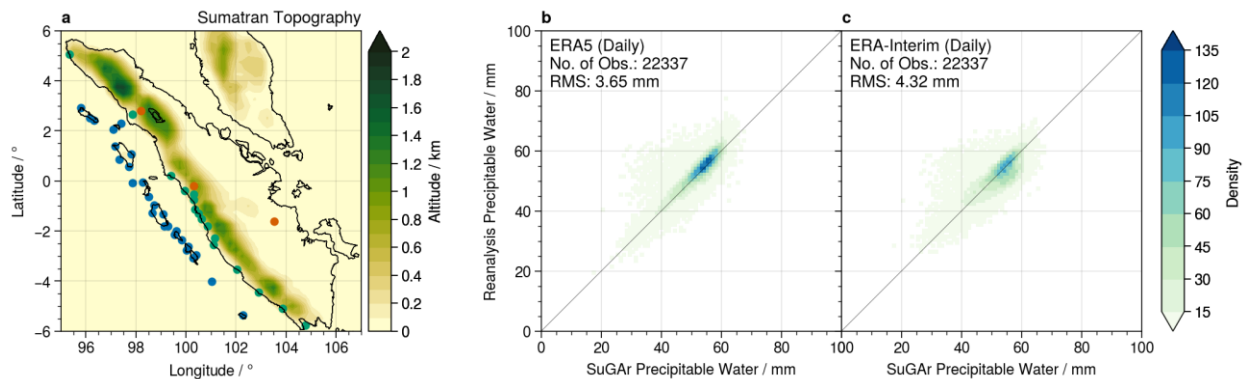178 1, 6, 7, 8 as suppressed phases over the MC.

179

180

Figure 1. (a) The GPS stations are divided into three categories: ocean (blue), coast (green), land
(red). The shading shows the orography. The comparison of PWV (b) between ERA5 and SuGAr
and (c) between ERA-Interim and SuGAr.

184 **3 Results**

185   3.1 Modulations of the diurnal cycle of PWV and rainfall by the MJO

186   Previous studies suggest that the diurnal cycle of precipitation and related sub-MJO-scale
187 features compete with the MJO for moist static energy, which may explain the MC barrier effect
188 (Neale & Slingo, 2003; Sakaeda et al., 2017; Ling et al., 2019). Here we extend the diurnal cycle
189 of PWV over Sumatra investigated by Torri et al. (2019) to the whole Maritime Continent and
190 also include the diurnal cycle of rainfall at different MJO phases. First we examine the diurnal
191 cycle of PWV over Sumatra with more coastal ground-based GPS stations compared to Fujita et
192 al. (2011). Figure S2 indicates that the diurnal cycle of PWV in this work has a clear sinusoidal
193 pattern, with a peak at about 19:00 local time, which is different from the midnight peak time
194 over the coastal stations in Fujita et al. (2011). With 6 years of data, the diurnal cycle of PWV
195 over Sumatra in our Figure 2 compares well with Torri et al. (2019)'s Fig. 11, which used 6
196 months of data to show that when the MJO transitions from suppressed to active phases, PWV
197 increases by roughly the same amount throughout the day across all surface types. The
198 modulation of the rainfall diurnal cycle by the MJO is substantial over both land and ocean, but
199 is stronger over the ocean than over the land (Figure 3). The diurnal cycles of rainfall and PWV
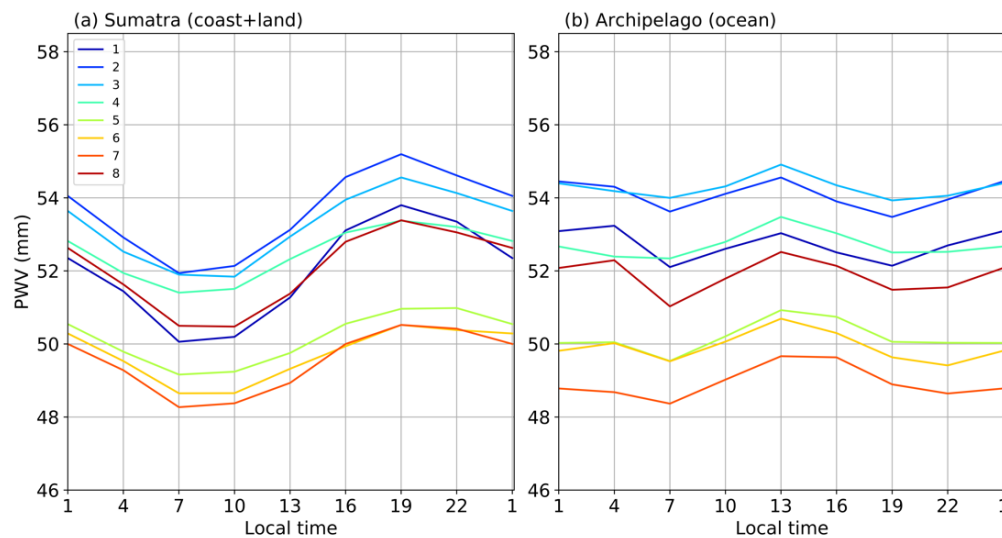200 over the whole Maritime Continent (Fig. S3&S4) show a similar behavior.

201

202
203 **Figure 2.** The diurnal cycle of precipitable water vapor over SuGAr stations (2008-2013) during
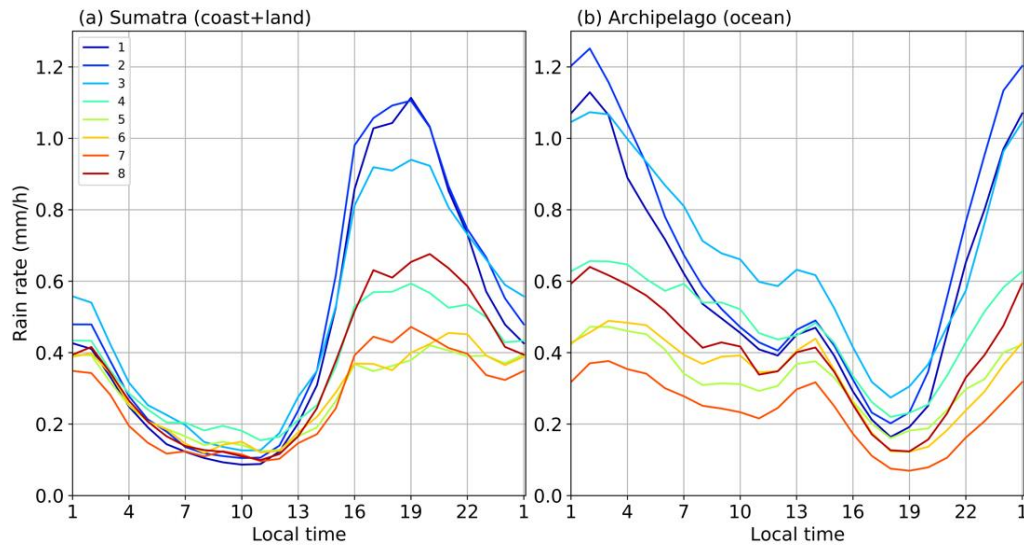204 MJO phases 1-8 (color), for (a) coast and land stations, and (b) ocean stations.

205

Figure 3. The diurnal cycle of precipitation rate over SuGAr stations (2008-2013) during MJO
phases 1-8 (color), for (a) coast and land stations, and (b) ocean stations.

208

209   3.2 Relationship between daily PWV and precipitation over the Maritime Continent

210   In this section, we examine how the relationship between the daily averaged PWV and
211   precipitation over land and ocean.

212   We first examine this relationship using Sumatra GPS data (Figure 4a). Across all surface
213   types (ocean, coast and land), the precipitation rate is on average below 0.5 mm/h when PWV is
214   below 55 mm. Over ocean, the rain-PWV relationship curve sharply increases when PWV is
215   above 55 mm, which is similar to what Bretherton et al. (2004) found over tropical oceans. At
216   the same time, when PWV is higher than 55 mm the precipitation rate over land is lower than
217   over the coast and much lower than over the ocean. The next question is, is Sumatra
218   representative of the broader MC area?

219   Figure 4b shows the relationship between PWV and rainfall over the MC using 12 years
220   of ERA5 PWV data and GPM IMERG precipitation data. Precipitation rate over the ocean
221   increases exponentially when PWV is above 55 mm, approaches 2 mm/h when PWV reaches 65
222   mm, which is similar to the results over Sumatra (Figure 4a). In contrast, the rain-PWV curves
223   over land and coast are less steep than that over ocean. At similar PWV values, the precipitation
224   rate over land is lower than over the ocean, which confirms a weaker rain dependence on PWV
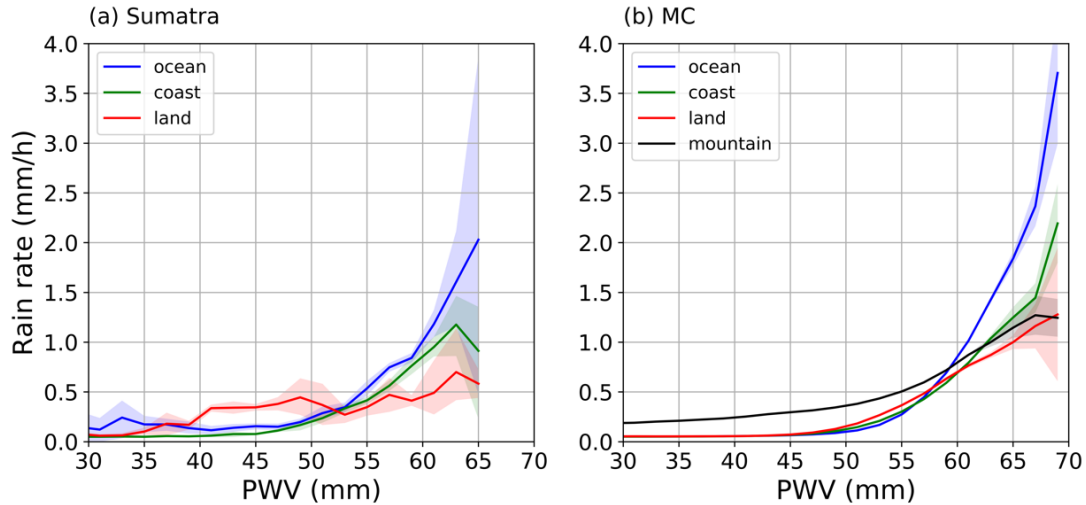225   over the Maritime Continent.

Figure 4. Relationship between daily rainfall and daily precipitable water vapor over (a) Sumatra and (b) the Maritime Continent, for oceanic areas (blue), coastal areas (green), land areas (red) and mountain areas (black). The shadings show the 95% confidence interval. Data are not shown above 65 mm for Sumatra (69 mm for the MC) due to limited occurrences of such high PWV values.

3.3 PWV and rainfall modulation by the MJO

Figure 5a shows the difference in the probability distribution functions (PDF) of daily-aggregated PWV between MJO active phases (Fig. S5a) and suppressed phases (Fig. S5b) over the Maritime continent. The difference in probability distribution of PWV shows a dipole pattern, corresponding to the PWV values shift between the different MJO phases. Except for the mountain grids, frequencies of PWV below (above) 57 mm decreased (increased), with a peak frequency decrease (increase) at 53mm (61 mm) with enhanced MJO convection. Note that this shift is remarkably similar over ocean, coast and land, except over mountainous regions, where the spectrum shifts to lower PWV values. Therefore the moisture mode associated with the MJO as measured by PWV is no weaker over the MC land compared to over the ocean.

Figure 5b shows the difference in the distributions of log precipitation rates between the active and suppressed MJO phases. This difference between the active phase and suppressed phase, is positive (negative) when precipitation rate is higher (lower) than about 0.5 mm/hr over all regions, corresponding to the strong convection during the active phase of the MJO over the MC. In contrast, the change in rainfall rate is larger over the ocean than over both land and coastal regions, which means the MJO modulation of precipitation rate is stronger over the surrounding ocean area than the MC. The frequency of high rainfall rates greater than 1 mm/hr is larger over ocean than land during the active MJO phases.

To summarize, the MJO has similar influences on PWV for different surface types, but has a weaker effect on the precipitation rate over land as compared to over the surrounding ocean area. This contrast between land and ocean, which is consistent with the weaker convection modulation over land found by Zhang & Ling (2017) and others, may be interpreted in terms of the difference in the sensitivity of rainfall on PWV between land and ocean.
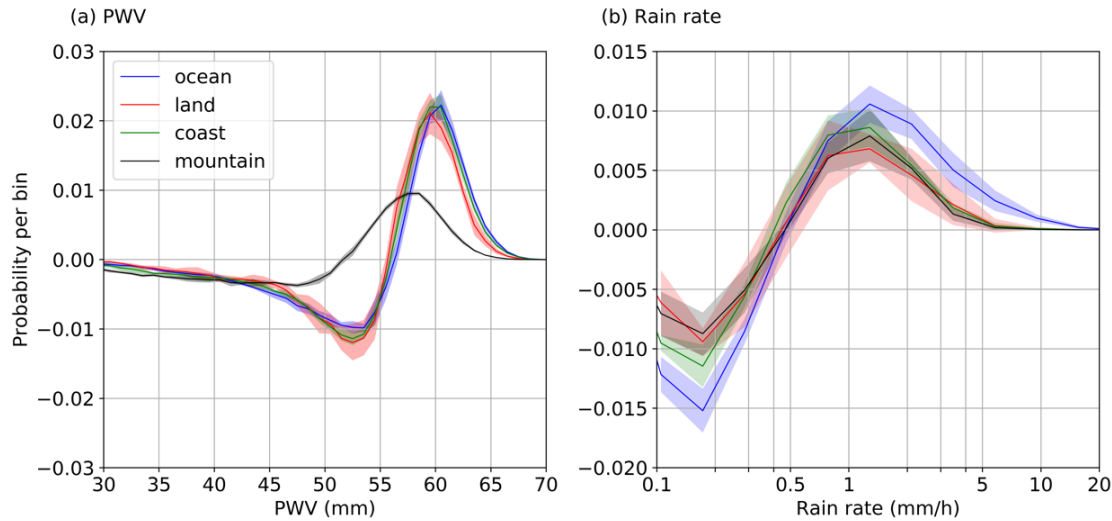
255

Figure 5. Difference of the distributions of (a) precipitable water vapor and (b) log rainfall rate
during the MJO active phases relative to the suppressed phases for ocean grids (blue), coast grids
(green), land grids (red) and mountain grids (black) over the MC. Bin size is 1mm for PWV and
0.217 in $\log_{10}$(precipitation rate) scale, respectively. Shadings show the 95% confidence interval.

4. Conclusions

This work is inspired by the "moisture mode" framework, in which the prognostic
moisture equation is the key to the MJO dynamics. One of the supporting evidence of the
"moisture mode" theory is the observed exponential rain-PWV relationship over the tropical
oceans (Bretherton et al., 2004), which shows that precipitation is highly sensitive to column
water vapor (or column relative humidity). In this work, we utilized the PWV derived from
ground-based GPS stations over Sumatra, which are unaffected by cloudy conditions or land-
surface emissivity, and extend the study to the whole MC with ERA5, which assimilates GPS
radio occultation data and shows good agreement with SuGAr.

We find a clear rain-PWV relationship over all surface types (i.e., ocean, land, and coast
areas), which is consistent with previous studies. However, the dependence of rainfall on PWV is
weaker over land and coast than over ocean. We also find that the MJO enhances the PWV by
roughly similar amounts over land and ocean, and suggest that the weaker modulation of rainfall
rate by the MJO over land compared to that over ocean may be a consequence of its weaker
dependence of rainfall on PWV. This in turn may lead to a weaker "moisture mode" that
partially explains the MC's barrier effect on the MJO. Whether and how a weaker rain-PWV
dependence over land is related to its stronger diurnal cycle will be further investigated through
numerical simulations in the future.

291

References:

293 Adames, Á. F., & Kim, D. (2016). The MJO as a dispersive, convectively coupled moisture
294   wave: Theory and observations. *Journal of the Atmospheric Sciences*, *73*(3), 913–941.
295   https://doi.org/10.1175/JAS-D-15-0170.1

296 Ahmed, F., & Schumacher, C. (2017). Geographical differences in the tropical precipitation-
297   moisture relationship and rain intensity onset. *Geophysical Research Letters*, *44*(2), 1114–
298   1122. https://doi.org/10.1002/2016GL071980

299 Andersen, J. A., & Kuang, Z. (2012). Moist static energy budget of MJO-like disturbances in the
300   atmosphere of a zonally symmetric aquaplanet. *Journal of Climate*, *25*(8), 2782–2804.
301   https://doi.org/10.1175/JCLI-D-11-00168.1

302 Arcodia, M. C., Kirtman, B. P., & Siqueira, L. S. P. (2020). How MJO Teleconnections and
303   ENSO Interference Impacts U.S. Precipitation. *Journal of Climate*, *33*(11), 4621–4640.
304   https://doi.org/10.1175/JCLI-D-19-0448.1

305 Askne, J., & Nordius, H. (1987). Estimation of tropospheric delay for microwaves from surface
306   weather data. *Radio Science*, *22*(03), 379–386. https://doi.org/10.1029/RS022i003p00379

307 Barrett, B. S. (2019). Connections between the Madden–Julian Oscillation and surface
308   temperatures in winter 2018 over eastern North America. *Atmospheric Science Letters*,
309   *20*(1), 1–8. https://doi.org/10.1002/asl.869

310 Bergemann, M., & Jakob, C. (2016). How important is tropospheric humidity for coastal rainfall
311   in the tropics ?, (May). https://doi.org/10.1002/2016GL069255.1.

312 Bretherton, C. S., Peters, M. E., & Back, L. E. (2004). Relationships between water vapor path
313   and precipitation over the tropical oceans. *Journal of Climate*, *17*(7), 1517–1528.
314   https://doi.org/10.1175/1520-0442(2004)017<1517:RBWVPA>2.0.CO;2

315 Feng, L., Hill, E. M., Banerjee, P., Hermawan, I., Tsang, L. L. H., Natawidjaja, D. H., et al.
316   (2015). A unified GPS-based earthquake catalog for the Sumatran plate boundary between
317   2002 and 2013. *Journal of Geophysical Research: Solid Earth*, *120*(5), 3566–3598.
318   https://doi.org/10.1002/2014JB011661

319 Fujita, M., Yoneyama, K., Mori, S., Nasuno, T., & Satoh, M. (2011). Diurnal convection peaks
320   over the eastern Indian Ocean off sumatra during different MJO phases. *Journal of the
321   Meteorological Society of Japan*, *89*(A), 317–330. https://doi.org/10.2151/jmsj.2011-A22

322 Hagos, S. M., Zhang, C., Feng, Z., Burleyson, C. D., De Mott, C., Kerns, B., et al. (2016). The
323   impact of the diurnal cycle on the propagation of Madden-Julian Oscillation convection

324   across the Maritime Continent. *Journal of Advances in Modeling Earth Systems*, *8*(4),
325   1552–1564. https://doi.org/10.1002/2016MS000725

326   Hersbach, H., Bell, B., Berrisford, P., Hirahara, S., Horányi, A., Muñoz-Sabater, J., et al. (2020).
327   The ERA5 global reanalysis. *Quarterly Journal of the Royal Meteorological Society*,
328   *146*(730), 1999–2049. https://doi.org/10.1002/qj.3803

329   Inness, P. M., & Slingo, J. M. (2006). The interaction of the Madden-Julian Oscillation with the
330   Maritime Continent in a GCM. *Quarterly Journal of the Royal Meteorological Society*,
331   *132*(618 A), 1645–1667. https://doi.org/10.1256/qj.05.102

332   Inness, P. M., Slingo, J. M., Guilyardi, E., & Cole, J. (2003). Simulation of the Madden-Julian
333   oscillation in a coupled general circulation model. Part II: The role of the basic state.
334   *Journal of Climate*, *16*(3), 365–382. https://doi.org/10.1175/1520-
335   0442(2003)016<0365:SOTMJO>2.0.CO;2

336   Kiladis, G. N., & Weickmann, K. M. (1992). Circulation Anomalies Associated with Tropical
337   Convection during Northern Winter. *Monthly Weather Review*, *120*(9), 1900–1923.
338   https://doi.org/10.1175/1520-0493(1992)120<1900:CAAWTC>2.0.CO;2

339   Ling, J., Zhang, C., Joyce, R., Xie, P. ping, & Chen, G. (2019). Possible Role of the Diurnal
340   Cycle in Land Convection in the Barrier Effect on the MJO by the Maritime Continent.
341   *Geophysical Research Letters*, *46*(5), 3001–3011. https://doi.org/10.1029/2019GL081962

342   Madden, R. A., & Julian, P. R. (1971). Detection of a 40–50 Day Oscillation in the Zonal Wind
343   in the Tropical Pacific. *Journal of the Atmospheric Sciences*, *28*(5), 702–708.
344   https://doi.org/10.1175/1520-0469(1971)028<0702:doadoi>2.0.co;2

345   Madden, R. A., & Julian, P. R. (1972). Description of Global-Scale Circulation Cells in the
346   Tropics with a 40–50 Day Period. *Journal of the Atmospheric Sciences*, *29*(6), 1109–1123.
347   https://doi.org/10.1175/1520-0469(1972)029<1109:DOGSCC>2.0.CO;2

348   Majda, A. J., & Yang, Q. (2016). A multiscale model for the intraseasonal impact of the diurnal
349   cycle over the maritime continent on the Madden-Julian oscillation. *Journal of the
350   Atmospheric Sciences*, *73*(2), 579–604. https://doi.org/10.1175/JAS-D-15-0158.1

351   Maloney, E. D., & Sobel, A. H. (2004). Surface fluxes and ocean coupling in the tropical
352   intraseasonal oscillation. *Journal of Climate*, *17*(22), 4368–4386.
353   https://doi.org/10.1175/JCLI-3212.1

354   Mo, K. C. (2000). Intraseasonal modulation of summer precipitation over North America.
355   *Monthly Weather Review*, *128*(5), 1490–1505. https://doi.org/10.1175/1520-
356   0493(2000)128<1490:IMOSPO>2.0.CO;2

357   Neale, R., & Slingo, J. (2003). The Maritime Continent and its role in the global climate: A
358   GCM study. *Journal of Climate*, *16*(5), 834–848. https://doi.org/10.1175/1520-
359   0442(2003)016<0834:TMCAIR>2.0.CO;2

360   Oda, T., Maksyutov, S., Andres, R. J., Office, A., Technology, E. S., Information, D., et al.
361   (2019). The Global Precipitation Measurement (GPM) mission's scientific achievements
362   and societal contributions: reviewing four years of advanced rain and snow observations,
363   *10*(1), 87–107. https://doi.org/10.5194/essd-10-87-2018.The

364   Rauniyar, S. P., & Walsh, K. J. E. (2011). Scale interaction of the diurnal cycle of rainfall over

the Maritime Continent and Australia: Influence of the MJO. *Journal of Climate*, *24*(2), 325–348. https://doi.org/10.1175/2010JCLI3673.1

Raymond, D. J. (2001). A New Model of the Madden – Julian Oscillation, 2807–2819.

Roundy, P. E., & Frank, W. M. (2004). Effects of low-frequency wave interactions on intraseasonal oscillations. *Journal of the Atmospheric Sciences*, *61*(24), 3025–3041. https://doi.org/10.1175/JAS-3348.1

Rui, H., & Wang, B. (1990). Development Characteristics and Dynamic Structure of Tropical Intraseasonal Convection Anomalies. *Journal of the Atmospheric Sciences*. https://doi.org/10.1175/1520-0469(1990)047<0357:dcadso>2.0.co;2

Sakaeda, N., Kiladis, G., & Dias, J. (2017). The diurnal cycle of tropical cloudiness and rainfall associated with the Madden-Julian oscillation. *Journal of Climate*, *30*(11), 3999–4020. https://doi.org/10.1175/JCLI-D-16-0788.1

Schreck, C. J., Cordeira, J. M., & Margolin, D. (2013). Which MJO events affect north american temperatures? *Monthly Weather Review*, *141*(11), 3840–3850. https://doi.org/10.1175/MWR-D-13-00118.1

Seo, K. H., Wang, W., Gottschalck, J., Zhang, Q., Schemm, J. K. E., Higgins, W. R., & Kumar, A. (2009). Evaluation of MJO forecast skill from several statistical and dynamical forecast models. *Journal of Climate*, *22*(9), 2372–2388. https://doi.org/10.1175/2008JCLI2421.1

Sobel, A., & Maloney, E. (2012). An idealized semi-empirical framework for modeling the Madden-Julian oscillation. *Journal of the Atmospheric Sciences*, *69*(5), 1691–1705. https://doi.org/10.1175/JAS-D-11-0118.1

Sobel, A., & Maloney, E. (2013). Moisture modes and the eastward propagation of the MJO. *Journal of the Atmospheric Sciences*, *70*(1), 187–192. https://doi.org/10.1175/JAS-D-12-0189.1

Tian, B., Waliser, D. E., & Fetzer, E. J. (2006). Modulation of the diurnal cycle of tropical deep convective clouds by the MJO. *Geophysical Research Letters*, *33*(20), 1–6. https://doi.org/10.1029/2006GL027752

Tippett, M. K. (2018). Robustness of relations between the MJO and U.S. tornado occurrence. *Monthly Weather Review*, *146*(11), 3873–3884. https://doi.org/10.1175/MWR-D-18-0207.1

Torri, G., Adams, D. K., Wang, H., & Kuang, Z. (2019). On the diurnal cycle of GPS-derived precipitable water vapor over sumatra. *Journal of the Atmospheric Sciences*, *76*(11), 3529–3552. https://doi.org/10.1175/JAS-D-19-0094.1

Vitart, F., & Molteni, F. (2010). Simulation of the Madden-Julian oscillation and its teleconnections in the ECMWF forecast system. *Quarterly Journal of the Royal Meteorological Society*, *136*(649), 842–855. https://doi.org/10.1002/qj.623

Wang, S., Sobel, A. H., Tippett, M. K., & Vitart, F. (2019). Prediction and predictability of tropical intraseasonal convection: seasonal dependence and the Maritime Continent prediction barrier. *Climate Dynamics*, *52*(9–10), 6015–6031. https://doi.org/10.1007/s00382-018-4492-9

Weaver, S. J., Wang, W., Chen, M., & Kumar, A. (2011). Representation of MJO Variability in

405   the NCEP Climate Forecast System. *Journal of Climate*, *24*(17), 4676–4694.
406   https://doi.org/10.1175/2011JCLI4188.1

407 Wheeler, M. C., & Hendon, H. H. (2004). An all-season real-time multivariate MJO index:
408   Development of an index for monitoring and prediction. *Monthly Weather Review*, *132*(8),
409   1917–1932. https://doi.org/10.1175/1520-0493(2004)132<1917:AARMMI>2.0.CO;2

410 Wu, C. H., & Hsu, H. H. (2009). Topographic influence on the MJO in the maritime continent.
411   *Journal of Climate*, *22*(20), 5433–5448. https://doi.org/10.1175/2009JCLI2825.1

412 Yamanaka, M. D. (2016). Physical climatology of Indonesian maritime continent: An outline to
413   comprehend observational studies. *Atmospheric Research*, *178–179*, 231–259.
414   https://doi.org/10.1016/j.atmosres.2016.03.017

415 Zhang, C. (2005). Madden Julian Oscillation Impacts. *Prediction Center.[Available Online at*
416   *Http …*, (2004), 4. https://doi.org/10.1029/2004RG000158.1.INTRODUCTION

417 Zhang, C., & Ling, J. (2017). Barrier effect of the Indo-Pacific Maritime Continent on the MJO:
418   Perspectives from tracking MJO precipitation. *Journal of Climate*, *30*(9), 3439–3459.
419   https://doi.org/10.1175/JCLI-D-16-0614.1

420 Zhou, Y., Lu, Y., Yang, B., Jiang, J., Huang, A., Zhao, Y., et al. (2016). On the relationship
421   between the Madden-Julian Oscillation and 2m air temperature over central Asia in boreal
422   winter. *Journal of Geophysical Research*, *121*(22), 13,250-13,272.
423   https://doi.org/10.1002/2016JD025651

424